IEEE Access
Multidisciplinary ⋮ Rapid Review ⋮ Open Access Journal

Received October 22, 2021, accepted November 10, 2021, date of publication November 16, 2021,
date of current version December 2, 2021.

Digital Object Identifier 10.1109/ACCESS.2021.3128763

Throughput Analysis in a Wireless Powered Mobile Communication System

PETROS S. BITHAS[1], (Senior Member, IEEE),
AND F. JAVIER LÓPEZ-MARTÍNEZ[2], (Senior Member, IEEE)
[1]General Department, National and Kapodistrian University of Athens, Psahna, 34400 Evia, Greece
[2]Communications and Signal Processing Laboratory, Instituto Universitario de Investigación en Telecomunicación (TELMA), Universidad de Málaga, CEI Andalucía TECH, ETSI Telecomunicación, 29010 Málaga, Spain

Corresponding author: Petros S. Bithas (pbithas@uoa.gr)

The work of F. Javier López-Martínez was supported in part by the Junta de Andalucia and the European Fund for Regional Development FEDER under Project P18-RT-3175, in part by the Agencia Estatal de Investigacion of Spain under Grant TEC2017-87913-R and Grant PID2020-118139RB-I00, and in part by the Instituto de Telecomunicación (TELMA).

ABSTRACT In this paper, important statistical characteristics of the ratio of double generalized-gamma random variables have been analytically evaluated. The derived results have been applied in a wireless powered mobile-to-mobile communication scenario, which operates in the presence of interference. The performance is investigated using the throughput criterion under two different scenarios, namely delay limited and delay tolerant transmissions. Moreover, since the links' reliability depends on the mobile nodes locations, the $2D$ Poisson point process is employed in order to more realistically model the physical layer behavior. The analytical results provided generalize previously reported ones, while the numerical results presented reveal the impact of various system's and channel's parameters, e.g., distance among nodes, interference, the non-linearity of the wireless medium.

INDEX TERMS Cascaded (double) generalized-gamma, Poisson point process, mobile-to-mobile communications, wireless powered communications.

I. INTRODUCTION

In mobile communication scenarios, in which both the transmitter (Tx) and the receiver (Rx) are in motion, a realistic model for the received amplitude behavior includes the product of fading amplitudes, as a result of the double-bouncing propagation mechanism [1]. Depending upon the propagation environment characteristics, various cascaded models have been investigated in the past, e.g., double-Nakagami [2] and the double-Weibull [3]. In addition to the physical justification, the cascaded fading models offer a good fit to experimental data related to mobile-to-mobile (M2M) communications [4].

Another parameter that affects the reliability of these systems is the locations of the Tx, Rx, and the interfering nodes. In this context, the stochastic geometry has been employed to faithfully model the locations of the wireless nodes as random point process, e.g., Poisson line process [5], Poisson point process (PPP) [6], double stochastic Poisson Line Cox Point (PLC) process [7]. For example in [7], the outage probability (OP) has been analyzed in a non-orthogonal multiple access (NOMA) vehicular communication system based on the PLC process. The outcome from these studies is that stochastic geometry is a useful tool to realistically model the geometrical patterns of the vehicles positions.

In practical scenarios, the M2M communication channel is also subject to co-channel interference due to the hidden terminal problem in contention-based accessing schemes, e.g., [8]–[11]. For example, in [10], assuming Nakagami-m fading channels, novel expressions for the OP of the signal-to-interference-plus-noise ratio (SINR) have been provided in a vehicular cooperative communication scenario. Moreover, in [9], the outage probability has been investigated in vehicular links assuming high signal-to-noise ratio (SNR) and weak interference scenarios. On the other hand, a promising technique that has gained the interest of the researchers and engineers is the energy harvesting (EH) from the radio frequency signals in an effort to increase the power of the (energy constrained) nodes [12]–[14]. A common approach in these papers is that the product and/or the ratio of random variables is required to be statistically investigated. More specifically, in [13], the statistical characterization of the

The associate editor coordinating the review of this manuscript and approving it for publication was Abderrahmane Lakas.

product of two $\kappa-\mu$ shadowed random variables (RVs) has been performed and applied to analyze the performance of a wireless powered communication (WPC) system. In [14], an EH mobile cooperative communication scenario has been investigated, in which the double-Rayleigh distribution has been adopted, and the symbol error rate has been evaluated.

In this paper, by generalizing previously reported results, the throughput of a wireless powered M2M communication (WPMC) system has been analytically investigated. To this aim, the double generalized-gamma (dGG) distribution has been employed, which is able to model a plethora of different mobile propagation conditions [15]. As a result, by exploiting the generic form of this distribution, various models are included as special cases. Moreover, the PPP is also adopted to model the mobile nodes' random locations. The main contributions are as follows:

- Novel expressions for important statistical characteristics of the ratio of independent but not identically distributed dGG RVs are provided. More specifically, the probability density function (PDF), the cumulative distribution function (CDF), the moment generating function (MGF), and the mean are derived;
- Novel expressions for the PDF and the CDF of the ratio of random distances in a PPP model are also evaluated;
- As an application example, a WPMC scenario has been considered, in which the throughput of delay limited transmission (DLT) and delay tolerant transmission (DTT) scenarios are analytically studied, by assuming deterministic locations for the mobile nodes;
- Finally, an approximate expression is also provided for the throughput, in a scenario, in which the locations of the mobile nodes are modeled as PPP.

The remainder of the paper is organized as follows. In Section II, important statistical metrics of the ratio of double GG RVs have been provided. In Section III, the statistics of the ratio of PPP have been analytical studied. In Section IV, the performance of WPMC scenario has been investigated in terms of the throughput, while in Section V several numerical evaluated results have been provided. Finally, Section VI concludes this paper.

II. STATISTICS OF THE RATIO OF DOUBLE GENERALIZED-GAMMA RVs

Let X_i denote a dGG RV with PDF given as [15]

$$f_{X_i}(x)=\frac{\Xi_i^{\frac{\theta_i^+}{2}}\beta_i x^{\beta_i\frac{\theta_i^+}{4}-1}}{\Gamma(m_i)\Gamma(m_{i+1})}K_{\theta_i^-}\left(2\sqrt{\Xi_i}x^{\frac{\beta_i}{4}}\right),\quad x\geq 0, \quad (1)$$

with $K_\nu(\cdot)$ denoting the νth order modified Bessel function of the second kind [16, eq. (8.407/1)] and $\Gamma(\cdot)$ the gamma function [16, eq. (8.310/1)]. Moreover, in (1), m_i, β_i are the distribution's shaping parameters, reflecting the clustering and non-linearity of the wireless medium, respectively, while $\bar{\gamma}_i$ denotes distribution's scaling parameter, related to the average SNR, $\Xi_x=\frac{m_x m_{x+1}}{\bar{\gamma}_x\bar{\gamma}_{x+1}}$, and $\theta_x^\pm=m_{x+1}\pm m_x$. It is noted that for $m_i=m_{i+1}=1$, (1) simplifies to the double-Weibull PDF, for $\beta_i=2$, it simplifies to the double-Nakagami, while for $m_i=m_{i+1}=1$ and $\beta_i=2$, it simplifies to the double-Rayleigh. Assuming integer values for m_{i+1},[1] the corresponding CDF is given by

$$F_{X_i}(x)=1-\sum_{k=0}^{m_{i+1}-1}\frac{2\Xi_i^{\frac{\mu_i^+}{2}}}{\Gamma(m_i)}x^{\frac{\beta_i}{4}(\mu_i^+)}K_{\mu_i^-}\left(2\sqrt{\Xi_i}x^{\frac{\beta_i}{4}}\right), \quad (2)$$

where $\mu_i^\pm=k\pm m_i$.

Theorem 1: Let Z denote the ratio of two independent dGG RVs, with PDF given in (1), i.e.,

$$Z=\frac{X_i}{X_j}. \quad (3)$$

The CDF of Z can be evaluated as[2]

$$F_Z(\gamma)=1-\sum_{k=0}^{m_{i+1}-1}\frac{\Xi_i^{\frac{\mu_i^+}{2}}/k!}{\Gamma(m_i)}\frac{\Xi_j^{\frac{\theta_j^+}{2}}\Xi_j^{-\xi_{i,j}}\beta_i^{\frac{\xi_{i,j}}{2}-1}}{\Gamma(m_j)\Gamma(m_{j+1})}\times\frac{\gamma^{\frac{\beta_i}{4}\mu_i^+}}{(2\pi)^{\beta_i+\beta_j-2}}G_{2\beta_i,2\beta_i}^{2\beta_j,2\beta_i}\left(\left(\frac{\Xi_i}{\beta_j^2}\right)^{\beta_j}\left(\frac{\beta_i^2}{\Xi_j}\right)^{\beta_i}\times\gamma^{\frac{\beta_i\beta_j}{2}}\middle|\begin{matrix}\Delta\left(\beta_i,1-\xi_{i,j}-\frac{\theta_j^-}{2}\right),\Delta\left(\beta_i,1-\xi_{i,j}+\frac{\theta_j^-}{2}\right)\\ \Delta\left(\beta_j,\frac{\mu_i^-}{2}\right),\Delta\left(\beta_j,-\frac{\mu_i^-}{2}\right)\end{matrix}\right), \quad (4)$$

where $\xi_{x,y}=\frac{\beta_x}{2\beta_y}(k+m_x)+\frac{m_y+m_{y+1}}{2}$, $\Delta(x,y)=\frac{y}{x},\frac{y+1}{x},\ldots,\frac{y+x-1}{x}$, and $G_{p,q}^{m,n}[\cdot|\cdot]$ denotes the Meijer's G-function [16, eq. (9.301)], which is a built-in function in many mathematical software packages, e.g., Mathematica. It is noted that for $m_i, m_j\to\infty$, (4) approximately simplifies to a previous reported result for the ratio of GG RVs [19].

Proof: The CDF of Z can be evaluated as

$$F_Z(\gamma)=\int_0^\infty F_{X_i}(\gamma x)f_{X_j}(x)dx. \quad (5)$$

Substituting (1) and (2) in (5), using the Meijer's G-function representation of the Bessel functions [20, eq. (14)] as well as [20, eq. (21)], (4) is deduced. ■

Assuming $\beta_i=\beta_j=\beta$, (4) simplifies to

$$F_Z(\gamma)=1-\sum_{k=0}^{m_{i+1}-1}\frac{1}{k!}\frac{\Xi_i^{\frac{\mu_i^+}{2}}}{\Gamma(m_i)}\frac{\Xi_j^{\frac{\theta_j^+}{2}}}{\Gamma(m_j)\Gamma(m_{j+1})}\times\frac{\gamma^{\frac{\beta}{4}\mu_i^+}}{\Xi_j^{\xi_{i,j}}}G_{2,2}^{2,2}\left(\frac{\Xi_i}{\Xi_j}\gamma^{\frac{\beta}{2}}\middle|\begin{matrix}1-\xi_{i,j}-\frac{\theta_j^-}{2},1-\xi_{i,j}+\frac{\theta_j^-}{2}\\ \frac{\mu_i^-}{2},-\frac{\mu_i^-}{2}\end{matrix}\right). \quad (6)$$

[1] This is a reasonable assumption since in practice, the measurement accuracy of the channel is sometimes only of integer order (for the fading parameter) of m_{i+1}. On the other hand, these results can be considered as upper/lower bounds for scenarios with non-integers values [17].

[2] An alternative representation could be obtained by using the results presented in [18].

Moreover, assuming $\Lambda(\gamma) = \left(\frac{\Xi_i}{\Xi_j}\gamma^{\frac{\beta}{2}}\right)$ and $\Lambda(\gamma) \to 0$, using [21, eq. (07.34.06.0006.01)], and after some mathematical simplifications, the following closed-form asymptotic expression for the CDF of Z is obtained

$$F_Z(\gamma) \approx 1 - \sum_{k=0}^{m_{i+1}-1} \frac{1}{k!}\frac{\Xi_i^k}{\Gamma(m_i)}\frac{\Xi_j^{\frac{\theta_j^+-\mu_i^-}{2}}}{\Gamma(m_j)\Gamma(m_{j+1})}\frac{\gamma^{\frac{\beta k}{2}}}{\Xi_j^{\xi_{i,j}}} \times \left[\Gamma\left(-\mu_i^-\right)\Gamma\left(\mu_{j+1}^+\right)\Gamma\left(\mu_j^+\right)(\Lambda(\gamma))^{\frac{\mu_i^-}{2}} - \Gamma\left(\mu_i^-\right)\Gamma\left(m_i+m_{j+1}\right)\Gamma\left(m_i+m_j\right)(\Lambda(\gamma))^{\frac{-\mu_i^-}{2}}\right]. \tag{7}$$

It is noted that (7) could be found useful in scenarios where high SNR investigations are performed.

Corollary 1.1: The PDF of Z is given by

$$f_Z(\gamma) = \frac{\Gamma\left(m_i+m_j\right)\Gamma\left(m_j+m_{i+1}\right)}{2\Xi_i^{m_{j+1}}\Gamma(m_i)\Gamma(m_{i+1})}\Xi_j^{m_{j+1}} \times \frac{\Gamma\left(m_i+m_{j+1}\right)\Gamma\left(m_{i+1}m_{j+1}\right)}{\Gamma(m_j)\Gamma(m_{j+1})}\frac{\beta}{\gamma^{m_{j+1}\frac{\beta}{2}+1}} \times {}_p\tilde{F}_q\left(m_i+m_{j+1}, m_{i+1}+m_{j+1}; \theta_i^+ + \theta_j^+; 1-\frac{\Xi_j}{\Xi_i\gamma^{\frac{\beta}{2}}}\right), \tag{8}$$

where ${}_p\tilde{F}_q(\cdot)$ denotes the regularized hypergeometric function [21, eq. (07.32.02.0001.01)].

Proof: The PDF of Z can be evaluated as

$$f_Z(\gamma) = \int_0^\infty x f_{X_i}(\gamma x) f_{X_j}(x) dx. \tag{9}$$

Substituting (1) in (9), using the Meijer's G-function representation of the Bessel functions [20, eq. (14)] as well as [20, eq. (21)], (8) is deduced. ∎

Corollary 1.2: The MGF of Z is given by

$$M_Z(s) = \frac{\beta^{\frac{1}{2}}2^{\theta_i^+ + \theta_j^+ - \beta - \frac{7}{2}}\left(\frac{\Xi_j}{\Xi_i}\right)^{m_{j+1}}\left(\frac{s}{\beta}\right)^{\frac{m_{j+1}\beta}{2}}}{\Gamma(m_i)\Gamma(m_{i+1})\Gamma(m_j)\Gamma(m_{j+1})\pi^{\beta+\frac{3}{2}}} \times G_{4,\beta+4}^{\beta+4,4}\left(\frac{\Xi_j^2 s^\beta}{\Xi_i^2\beta^\beta}\middle| \begin{matrix}\Delta(2,1-m_i-m_{j+1}), \Delta(2,1-m_{i+1}-m_{j+1}) \\ \Delta\left(\beta, \frac{-m_{j+1}\beta}{2}\right), 0, \frac{1}{2}, \Delta(2, m_j-m_{j+1})\end{matrix}\right). \tag{10}$$

Proof: For evaluating the MGF of Z, (8) is substituted in the definition of the MGF, i.e., $M_Z(s) \triangleq \mathbb{E}\{\exp(-s\gamma)\}$, with $\mathbb{E}\{\cdot\}$ denoting expectation. Using [22, eq. (3.37.2/1)] in this definition and after some mathematical analysis, (10) is deduced. ∎

Corollary 1.3: The mean value of Z is given by

$$\bar{Z} = \frac{\Gamma(m_i+m_j)\Gamma(m_j+m_{i+1})\Gamma(m_{j+1}-\frac{2}{\beta})}{\Gamma(m_i)\Gamma(m_j)\Gamma(m_{i+1})\Gamma(m_{j+1})} \times \left(\frac{\Xi_j}{\Xi_i}\right)^{\frac{2}{\beta}}\frac{\Gamma(m_i+\frac{2}{\beta})\Gamma(m_{i+1}+\frac{2}{\beta})\Gamma(m_j-\frac{2}{\beta})}{\Gamma(m_j+m_{i+1})\Gamma(m_i+m_j)}. \tag{11}$$

Proof: For evaluating $\bar{Z}$, (8) is substituted in $\bar{Z} \triangleq \mathbb{E}\{\gamma\}$ and by using [22, eq. (2.21.1/2)] in this definition and after some analytical steps, (11) is deduced. ∎

III. ON THE STATISTICS OF THE RATIO OF RANDOM DISTANCES IN A PPP

In this section, assuming a PPP model, important statistical characteristics of the ratio of random distances are analytically investigated. Let R_i denoting the distance between a point and its nth nearest neighbour in a PPP in $\mathbb{R}^m$. The PDF of R_i is [23]

$$f_{R_i}(r) = \frac{m(\lambda c_m r^m)^n}{r\Gamma(n)}\exp\left(-\lambda c_m r^m\right), \tag{12}$$

where λ denotes the node's spatial density, while $c_m = \frac{\pi^{m/2}}{(m/2)!}$ if m is even or $c_m = \frac{\pi^{(m-1)/2}2^m}{m!}\frac{m-1}{2}$ if m is odd. The corresponding CDF expression is given by

$$F_{R_i}(r) = \frac{\gamma(n, \lambda c_m r^m)}{\Gamma(n)}, \tag{13}$$

where $\gamma(\cdot,\cdot)$ denotes the lower incomplete gamma function [16, eq. (8.350/1)].

Proposition 1: Let $Y = \frac{R_i}{R_j}$ denote a RV defined as the ratio of two independent random distances each of them following the PDF given in (12). The CDF of Y is given by

$$F_Y(r) = \frac{r^{mn}}{\Gamma(n)^2}\frac{\Gamma(2n)/n}{(1+r^m)^{2n}}{}_2F_1\left(1, 2n; n+1; \frac{r^m}{r^m+1}\right), \tag{14}$$

where ${}_2F_1(\cdot)$ denotes the Gauss hypergeometric function [16, eq. (9.100)].

Proof: By substituting (12) and (13) in the definition of the ratio of two RVs given in (5) and using [16, eq. (6.455/2)], (14) is extracted and this completes the proof. ∎

Based on (14), the corresponding PDF expression can be directly evaluated as

$$f_Y(r) = \frac{m\Gamma(2n)}{\Gamma(n)^2}\frac{r^{mn-1}}{(1+r^m)^{2n}}. \tag{15}$$

The mean value of Y can be evaluated by substituting (15) in $\bar{Y} \triangleq \mathbb{E}\{r\}$ and using [16, eq. (3.251/11)], resulting to

$$\bar{Y} = \frac{\Gamma(n-1/m)\Gamma(n+1/m)}{\Gamma(n)^2}. \tag{16}$$

It is worth-noting that the node spatial density λ does not influence the expectation of the ratio of the two random distances in a PPP model.

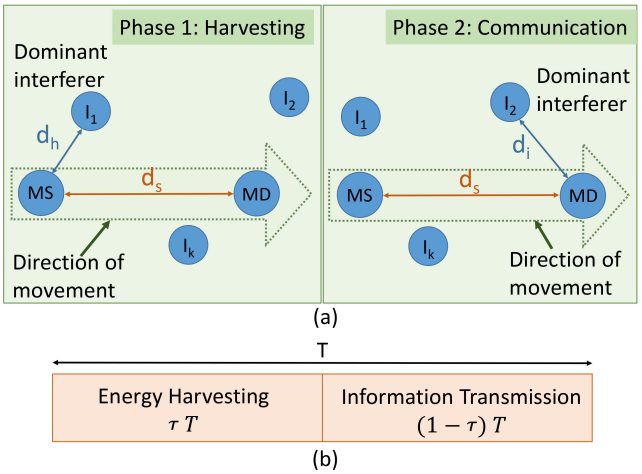

FIGURE 1. (a) System model under consideration; (b) Time switching operations for energy harvesting and information processing.

IV. WIRELESS POWERED M2M COMMUNICATION SYSTEMS APPLICATION EXAMPLE

The previous presented analytical framework can be applied in various wireless communication scenarios, in which the ratio of dGG RVs is observed. Here, as an application example, a throughput analysis of a WPMC system is performed. In this context, the system model under investigation includes a mobile-source (*MS*) that communicates with the mobile-destination (*MD*) in the presence of a dominant mobile-interferer (*I*),[3] all equipped with single antennas. The system model under consideration is given in Fig. 1(a). In this figure, the subscripts s, h, i denote the parameters related to *MS*-*MD*, *I*-*MS*, *I*-*MD*, respectively. Moreover, the *MS* is assumed to be energy-constrained and thus it harvests the transmitted energy from *I* (or other transmitting source). Assuming T is the duration of a block, in the first phase of transmission, *MS* harvests energy in an interval τT, where $0 < \tau < 1$ [12]. Under this scenario, the harvested energy at the *MS* is given by

$$E_h = \frac{\eta \tau T P_h g_h}{d_h^a}, \tag{17}$$

where $0 < \eta < 1$ is the energy conversion coefficient, P_h is the transmission power of the nearest interferer at this phase *I*, g_h follows the PDF given in (1), and d_h denotes the distance between *I* and *MS*. In the second phase of communication, the information is transmitted in the rest of the block, i.e., $(1-\tau)T$, while the *MD* is also experiencing interference (from the same with the first phase node or other nearby). The time-switching operation between EH and information processing procedures is depicted in Fig. 1(b). Moreover, it is assumed that the level of interference is such that the effect of thermal noise on system's performance can be ignored. Certainly, such a scenario is less generic; however, it has clear practical interest and importance and this is the reason why it has been studied many times in the past, e.g., [12]. Therefore, in this interference limited scenario, the received signal-to-interference ratio (SIR) at the *MD* is given by [12]

$$\gamma = \frac{\eta \tau P_h g_h g_s d_i^a}{(1-\tau) P_i g_i d_h^a d_s^a}. \tag{18}$$

In (18), g_s, g_i denote the square amplitude coefficients of the channel for the $MS-MD$ and $I-MD$ links, respectively, both following (1), d_s, d_i denote the distances between $MS-MD$ and $I-MD$, respectively, and P_i denotes the transmit power for *I* at the second phase. Under the assumption of a DLT scenario and a constant transmission rate R, the average throughput can be expressed as

$$R_{DL}(\tau) = (1 - P_{out})\, R(1-\tau), \tag{19}$$

with P_{out} denoting the OP of the system under consideration. Regarding DTT scenario, the throughput of the system is given by

$$\begin{aligned} R_{DT}(\tau) &= (1-\tau)\mathbb{E}\left\langle \log_2(1+\gamma)\right\rangle \\ &\overset{(\alpha)}{<} (1-\tau)\log_2(1+\mathbb{E}\left\langle\gamma\right\rangle). \end{aligned} \tag{20}$$

In (20), (α) is due to the Jensen's inequality. For evaluating the throughput for both DLT and DTT scenarios, expressions for the OP and the moments should, respectively, be extracted.

A. DETERMINISTIC DISTANCES

In this subsection the performance of the system under consideration has been investigated under the assumption of deterministic distances among the nodes. For evaluating the OP, the following proposition will be exploited

Proposition 2: Let $W = Z \cdot X_z$, with Z, X_z are RVs with CDF and PDF given in (6) and (1), respectively, assuming equal values for β. The CDF of W can be derived as

$$\begin{aligned} &F_W(\gamma) \\ &= 1 - \sum_{k=0}^{m_{i+1}-1} \frac{\Xi_j^{\frac{\theta_z^+}{2}} \Xi_z^{\frac{\theta_z^+}{2}} \Xi_i^{\frac{\theta_z^+}{2}} / k!}{\Gamma(m_i)\Gamma(m_j)\Gamma(m_{j+1})\Gamma(m_z)} \\ &\quad \times \frac{\gamma^{\frac{\beta}{4}\theta_z^+}}{\Gamma(m_{z+1})} G_{2,4}^{4,2}\left(\frac{\Xi_i \Xi_z}{\Xi_j}\gamma^{\frac{\beta}{2}} \middle| \begin{matrix} 1-\frac{\theta_z^+}{2}-m_j, 1-\frac{\theta_z^+}{2}-m_{j+1} \\ \frac{\theta_z^-}{2}, -\frac{\theta_z^-}{2}, -\frac{\theta_z^+}{2}+k, -\frac{\theta_z^+}{2}+m_i \end{matrix}\right). \end{aligned} \tag{21}$$

Proof: The CDF of W can be evaluated as $F_W(\gamma) = \int_0^\infty F_Z(\gamma/x) f_{X_z}(x) dx$. Substituting (6) and (1) in this definition and using [20, eq. (21)], (21) is finally deduced. ■

The P_{out} can be evaluated as follows

$$\begin{aligned} P_{out} &= \Pr\left\{\log_2(1+\gamma) < R\right\} = \Pr\left\{\gamma < \gamma_{th}\right\} \\ &= \Pr\left\{W < A_{th}\right\} = F_W(A_{th}), \end{aligned} \tag{22}$$

where $Pr\{\cdot\}$ denotes probability, $\gamma_{th} = 2^R - 1$, and $A_{th} = \frac{(1-\tau)P_i d_h^a d_s^a \gamma_{th}}{\eta \tau P_h d_i^a}$. Using (21)[4] in (22), the following exact

[3] This assumption is quite common in the open technical literature since it facilitates the analysis in scenarios where the aggregated interference can be considered as low enough to be negligible [24].

[4] Without loss of the generality, for all dGG RVs, normalized to one scaling parameters have been considered.

analytical expression for the OP is obtained

$$P_{out} = F_\gamma(\gamma_{th}) = 1 - \sum_{k=0}^{m_{s+1}-1} \frac{\Xi_i^{\frac{\theta_h^+}{2}} \Xi_s^{\frac{\theta_h^+}{2}} \Xi_h^{\frac{\theta_h^+}{2}} / k!}{\Gamma(m_s)\Gamma(m_i)\Gamma(m_{i+1})\Gamma(m_h)} \times \frac{A_{th}^{\frac{\beta}{4}\theta_h^+}}{\Gamma(m_{h+1})} G_{2,4}^{4,2}\left(\frac{\Xi_s \Xi_h}{\Xi_i} A_{th}^{\beta/2} \middle| \begin{matrix} 1-\frac{\theta_h^+}{2}-m_i, 1-\frac{\theta_h^+}{2}-m_{i+1} \\ \frac{\theta_h^-}{2}, -\frac{\theta_h^-}{2}, -\frac{\theta_h^+}{2}+k, -\frac{\theta_h^+}{2}+m_s \end{matrix} \right). \quad (23)$$

The mean value of γ in (18) is defined as $\bar{\gamma} = \int_0^\infty \gamma f_\gamma(\gamma) d\gamma$. By employing the integration by parts in this definition, i.e., $\int_a^b \gamma F'_\gamma(\gamma) d\gamma = \gamma F_\gamma(\gamma)\Big]_b^a - \int_a^b F_\gamma(\gamma) d\gamma$, and after some mathematical simplifications, it results to the following CDF-based definition for the expectation of γ

$$\bar{\gamma} = \int_0^\infty \left(1 - F_\gamma(\gamma)\right) d\gamma. \quad (24)$$

Substituting (23) in this definition, using [20, eq. (21)], and after some mathematical manipulations, finally yields to the following closed-form expression for $\bar{\gamma}$

$$\bar{\gamma} = \sum_{k=0}^{m_{s+1}-1} \frac{\Xi_i^{-\frac{\theta_h^+}{2}} \Xi_s^{\frac{\theta_h^+}{2}} / k!}{\Gamma(m_s)\Gamma(m_i)\Gamma(m_{i+1})} \frac{2\Xi_h^{\frac{\theta_h^+}{2}} / \beta}{\Gamma(m_h)\Gamma(m_{h+1})} \times \Gamma\left(\frac{2}{\beta}+k\right)\Gamma\left(\frac{2}{\beta}+m_s\right)\Gamma\left(\frac{2}{\beta}+m_h\right) \times \left(\frac{2}{\beta}+m_{h+1}\right)\Gamma\left(\frac{\theta_h^+}{2}+m_i\right)\Gamma\left(\frac{\theta_h^+}{2}+m_{i+1}\right) \times A_{th}^{\frac{\beta}{4}\theta_h^+ + 1}\left(A_{th}\frac{\Xi_s\Xi_h}{\Xi_i}\right)^{-\frac{2}{\beta}-\frac{\theta_h^+}{2}}. \quad (25)$$

B. RANDOM DISTANCES

In this section, it is assumed that the location of both the node that transfers power, d_h, and the interferer, d_i, are modeled as independent homogeneous $2-D$ PPP of intensity λ.[5] Under this scenario, the CDF expression in (23) is conditioned on the ratio d_h/d_i which defines a new RV with PDF given in (15). In order to remove this conditioning, (23) and (15) should be included in an integral of the form given in (5). However, by making this substitution, an exact closed-form solution to this integral cannot be obtained. Therefore, for numerically evaluating the OP, the Gauss-Laguerre quadrature is employed as follows [26]

$$P_{out} \cong \sum_{i=1}^{n} w_i \exp(x_i) F_\gamma(x_i) f_Y(x_i), \quad (26)$$

where the abscissas and weights, x_i, w_i, respectively, can be found in [26, Table 25.9]. After numerically approximating the P_{out}, the throughput for the DLT scenario can be directly evaluated using (26) in (19). It is noted that the result presented in (26) could be also considered as an upper bound for the OP in a scenario, where dependency exists between the distances d_i, d_h in (18). Moreover, it is noteworthy that the numerical evaluation of the OP in (26) can only be performed by exploiting the results given in (23) and (15).

[5]The distance between the *MS* and *MD* is considered to be constant modeling for example a scenario in which *MS*, *MD* are members of a vehicle-to-vehicle platoon group [25].

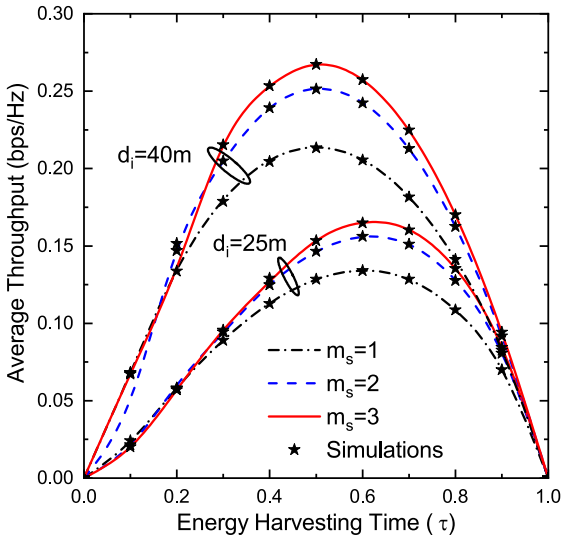

FIGURE 2. Deterministic locations: Throughput of DLT vs the EH time τ for different values of m_s.

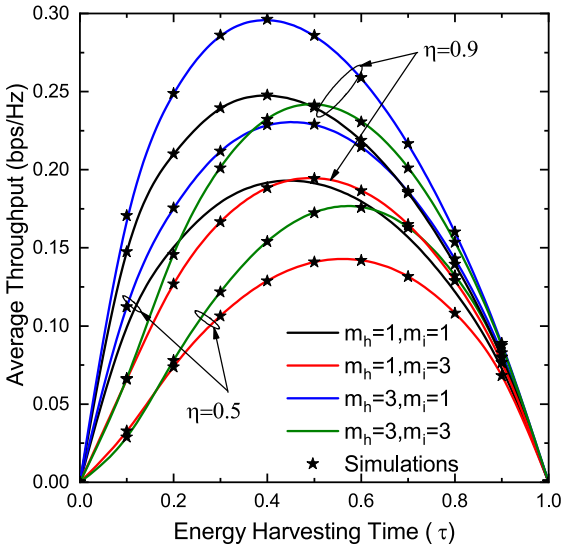

FIGURE 3. Deterministic locations: Throughput of DLT vs the EH time τ for different values of m_h, m_i.

V. NUMERICAL RESULTS

In this section, the theoretical results are verified through Monte Carlo simulations, which have been obtained by averaging 10^6 independent trials. Unless otherwise stated, it is assumed $R = 1$ bps/Hz, i.e., $\gamma_{th} = 1$, $\beta = 2.5$, $d_s = 10$m, and $\alpha = 1.8$.[6] In all the figures, the throughput has

[6]The simulation parameters considered here represent typical values for various short range mobile communication scenarios, e.g., [27], [28].

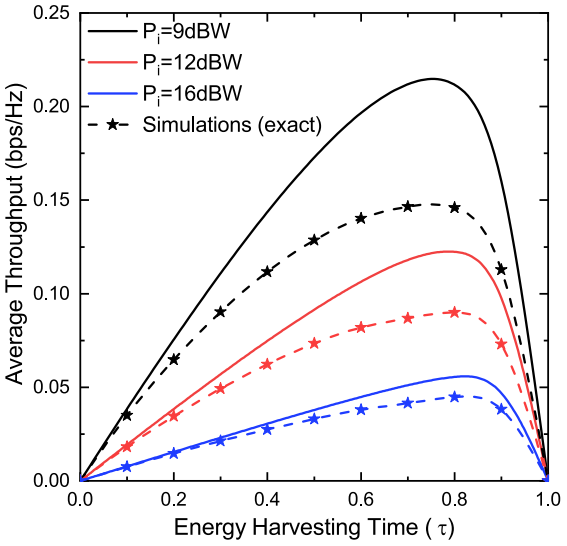

FIGURE 4. Deterministic locations: Throughput of DTT vs the EH time τ for different values of P_i.

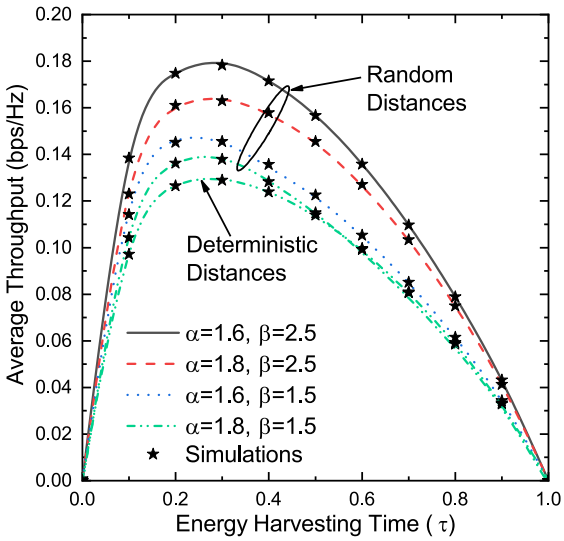

FIGURE 5. Stochastic locations: Throughput of DLT vs the EH time τ for different values of α and β.

been evaluated as a function of the energy harvesting time τ. In Fig. 2, a DLT scenario has been assumed and the following parameters were used in (23): $m_i = m_h = 2$, $\eta = 0.7$, $d_h = 5$m, $P_i = 7dBW$, $P_h = 12dBW$. As it is shown in this figure, the performance improves as the channel conditions of the $MS - MD$ link get better, i.e., m_s increases. However, the improvement decreases as m_s increases. Moreover, the difference among the performances increases for larger values of the interfering node distance d_i. It is also interesting to be noted that variations on d_i result to different EH intervals τ that offer the best throughput values. In Fig. 3, also DLT scenario has been assumed and the following parameters were used in (23): $m_s = 1$, $d_h = 5$m, $d_i = 40$m, $P_i = 7dBW$, $P_h = 12dBW$. As it is shown, the best performance is obtained by assuming mild fading conditions for the EH link and severe for the interfering, while the worst for the opposite scenario. It is noted that the performance is better in scenarios with bad channel conditions in both links as compared to the ones with good channel conditions, which reveals the increased impact of the interference to the system's performance. This difference is more clearly observed at the low energy coefficient values.

In Fig. 4, a DTT scenario has been assumed and the following parameters were used in (20) and (25): $m_s = m_i = m_h = 2$, $d_h = d_s = 10$m, $d_i = 30$m, $P_h = 12dBW$. As it is shown, a considerable reduction on the performance is obtained as the interferer's transmit power P_i increases. It is important to mention that the upper bound becomes more tight for higher values of P_i, while the gap among the exact results and the ones based on the bound is due to Jensen's property. Finally, in Fig. 5, focusing on the stochastic distances case, assuming a DLT scenario, and with the aid of (26), the following parameters were set: $m_s = m_i = m_h = 1$, $R = 0.5$ bps/Hz, i.e., $\gamma_{th} = 0.4$, $d_s = 5$m, $P_i = 0dBW$, $P_h = 15dBW$, while $n = 50$. As it is shown in this figure, the performance decreases as α increases, while as the non-linearity of the medium becomes less severe, i.e., assuming higher values of β, the performance gets better. It is interesting to be noted that the analytical approximated results are quite close to the simulated ones. Moreover, in this figure, the corresponding performance of a scenario with deterministic distances is also included, with $d_i = d_h = 20$m. As it is seen, for similar channel conditions and average distances, the deterministic scenario provides a pessimistic result of the throughput and thus can be considered as a lower bound to the random one. In all cases, the simulation results that have been included conform to the analytical ones.

VI. CONCLUSION

In this paper, a throughput analysis of a wireless powered M2M communication scenario has been performed. Towards this objective, important statistical metrics of the ratio of dGG RVs have been evaluated, such as the PDF, CDF, and the MGF. The presented analysis generalizes previously reported results, while it also takes into account the stochastic behavior of the distance among the nodes. It is revealed the important impact of i) the interference, ii) the non-linear behavior of the wireless medium, and iii) the impact of the position randomness, on the system's performance.

REFERENCES

[1] J. Salo, H. M. El-Sallabi, and P. Vainikainen, "Statistical analysis of the multiple scattering radio channel," *IEEE Trans. Antennas Propag.*, vol. 54, no. 11, pp. 3114–3124, Nov. 2006.

[2] G. K. Karagiannidis, N. C. Sagias, and P. T. Mathiopoulos, "N*Nakagami: A novel stochastic model for cascaded fading channels," *IEEE Trans. Commun.*, vol. 55, no. 8, pp. 1453–1458, Aug. 2007.

[3] P. S. Bithas, A. G. Kanatas, D. B. da Costa, and P. K. Upadhyay, "Transmit antenna selection in vehicle-to-vehicle time-varying fading channels," in *Proc. IEEE Int. Conf. Commun. (ICC)*, May 2017, pp. 1–6.

[4] V. Erceg, S. J. Fortune, J. Ling, A. J. Rustako, and R. A. Valenzuela, "Comparisons of a computer-based propagation prediction tool with experimental data collected in urban microcellular environments," *IEEE J. Sel. Areas Commun.*, vol. 15, no. 4, pp. 677–684, May 1997.

[5] V. V. Chetlur and H. S. Dhillon, "Coverage and rate analysis of downlink cellular vehicle-to-everything (C-V2X) communication," *IEEE Trans. Wireless Commun.*, vol. 19, no. 3, pp. 1738–1753, Mar. 2020.
[6] A.-K. Ajami and H. Artail, "Analyzing the impact of the coexistence with IEEE 802.11 ax Wi-Fi on the performance of DSRC using stochastic geometry modeling," *IEEE Trans. Commun.*, vol. 67, no. 9, pp. 6343–6359, Sep. 2019.
[7] Y. Sun, Z. Ding, X. Dai, K. Navaie, and D. K. C. So, "Performance of downlink NOMA in vehicular communication networks: An analysis based on Poisson line cox point process," *IEEE Trans. Veh. Technol.*, vol. 69, no. 11, pp. 14001–14006, Nov. 2020.
[8] J. Lee, J. H. Lee, and S. Bahk, "Performance analysis for multi-hop cognitive radio networks over cascaded Rayleigh fading channels with imperfect channel state information," *IEEE Trans. Veh. Technol.*, vol. 68, no. 10, pp. 10335–10339, Oct. 2019.
[9] Y. Ni, Y. Liu, Q. Wang, Y. Wang, H. Zhao, and H. Zhu, "Vehicular networks under Nakagami-m fading channels: Outage probability and ergodic achievable rate," *IEEE Access*, vol. 8, pp. 121501–121512, 2020.
[10] K. Eshteiwi, G. Kaddoum, B. Selim, and F. Gagnon, "Impact of co-channel interference and vehicles as obstacles on full-duplex V2V cooperative wireless network," *IEEE Trans. Veh. Technol.*, vol. 69, no. 7, pp. 7503–7517, Jul. 2020.
[11] G. Ghatak, "Cooperative relaying for URLLC in V2X networks," *IEEE Wireless Commun. Lett.*, vol. 10, no. 1, pp. 97–101, Jan. 2021.
[12] Y. H. Al-Badarneh, C. N. Georghiades, and M.-S. Alouini, "On the throughput of interference-based wireless powered communications with receive antenna selection," *IEEE Trans. Veh. Technol.*, vol. 69, no. 3, pp. 3048–3056, Mar. 2020.
[13] U. Fernandez-Plazaola, L. Moreno-Pozas, F. J. Lopez-Martinez, J. F. Paris, E. Martos-Naya, and J. M. Romero-Jerez, "A tractable product channel model for line-of-sight scenarios," *IEEE Trans. Wireless Commun.*, vol. 19, no. 3, pp. 2107–2121, Mar. 2020.
[14] B. C. Nguyen, T. M. Hoang, V. T. Nguyen, C. T. Phuong, and L. T. Dung, "Symbol error rate of energy harvesting full-duplex relay systems over cascade Rayleigh fading channels," in *Proc. Int. Conf. Comput. Commun. Technol. (RIVF)*, Oct. 2020, pp. 1–5.
[15] P. S. Bithas, A. G. Kanatas, D. B. da Costa, P. K. Upadhyay, and U. S. Dias, "On the double-generalized gamma statistics and their application to the performance analysis of V2V communications," *IEEE Trans. Commun.*, vol. 66, no. 1, pp. 448–460, Jan. 2018.
[16] I. S. Gradshteyn and I. M. Ryzhik, *Table of Integrals, Series, and Products*, 6th ed. New York, NY, USA: Academic, 2000.
[17] V. Aalo and J. Zhang, "Performance analysis of maximal ratio combining in the presence of multiple equal-power cochannel interferers in a Nakagami fading channel," *IEEE Trans. Veh. Technol.*, vol. 50, no. 2, pp. 497–503, Mar. 2001.
[18] E. J. Leonardo, M. D. Yacoub, and R. A. de Souza, "Ratio of products of α-μ variates," *IEEE Commun. Lett.*, vol. 20, no. 5, pp. 1022–1025, May 2016.
[19] E. J. Leonardo, D. B. da Costa, U. S. Dias, and M. D. Yacoub, "The ratio of independent arbitrary α-μ random variables and its application in the capacity analysis of spectrum sharing systems," *IEEE Trans. Commun.*, vol. 16, no. 11, pp. 1776–1779, Nov. 2012.
[20] V. S. Adamchik and O. I. Marichev, "The algorithm for calculating integrals of hypergeometric type functions and its realization in REDUCE system," in *Proc. Int. Symp. Symbolic Algebr. Comput.*, Tokyo, Japan, 1990, pp. 212–224.
[21] (2021). *The Wolfram Functions Site*. [Online]. Available: http://functions.wolfram.com
[22] A. Prudnikov, Y. Brychkov, and O. Marichev, *Integrals and Series*. New York, NY, USA: Gordon and Breach, 1986.
[23] M. Haenggi, "On distances in uniformly random networks," *IEEE Trans. Inf. Theory*, vol. 51, no. 10, pp. 3584–3586, Oct. 2005.
[24] M. A. M. Hassanien and P. Loskot, "Assessment of the link performance with a single interferer," *IEEE Trans. Veh. Technol.*, vol. 62, no. 3, pp. 1373–1377, Mar. 2013.
[25] J. Mei, K. Zheng, L. Zhao, L. Lei, and X. Wang, "Joint radio resource allocation and control for vehicle platooning in LTE-V2V network," *IEEE Trans. Veh. Technol.*, vol. 67, no. 12, pp. 12218–12230, Dec. 2018.
[26] M. Abramowitz and I. A. Stegun, *Handbook of Mathematical Functions: With Formulas, Graphs, and Mathematical Tables*, vol. 55. Chelmsford, MA, USA: Courier Corporation, 1964.
[27] H. Fernández, L. Rubio, V. M. Rodrigo-Peñarrocha, and J. Reig, "Path loss characterization for vehicular communications at 700 MHz and 5.9 GHz under LOS and NLOS conditions," *IEEE Antennas Wireless Propag. Lett.*, vol. 13, pp. 931–934, 2014.
[28] P. Raut, P. K. Sharma, T. A. Tsiftsis, and Y. Zou, "Power-time splitting-based non-linear energy harvesting in FD short-packet communications," *IEEE Trans. Veh. Technol.*, vol. 69, no. 8, pp. 9146–9151, Aug. 2020.

PETROS S. BITHAS (Senior Member, IEEE) received the Diploma degree in electrical and computer engineering and the Ph.D. degree in wireless communication system from the University of Patras, Greece, in 2003 and 2009, respectively. Since November 2010, he has been an Associate Researcher with the Department of Digital Systems, University of Piraeus (UNIPI), Greece, where he participates in a number of R&D projects. He is currently an Assistant Professor with the General Department, National and Kapodistrian University of Athens, Greece. He has published more than 40 articles in international scientific journals and 39 articles in the proceedings of international conferences. His current research interests include stochastic modeling of wireless communication channels and design and performance analysis of vehicular communication systems. He has been selected as an Exemplary Reviewer of IEEE Communications Letters, in 2010 and 2019, and IEEE Transactions on Communications, in 2020. He serves on the Editorial Board of the *International Journal of Electronics and Communications*, (Elsevier) and Telecom, Drones (MDPI).

F. JAVIER LÓPEZ-MARTÍNEZ (Senior Member, IEEE) received the M.Sc. and Ph.D. degrees in telecommunication engineering from the University of Malaga, Spain, in 2005 and 2010, respectively. He was an Associate Researcher with the Communication Engineering Department, University of Malaga, between 2005 and 2012. He was a Marie Curie Postdoctoral Fellow with the Wireless Systems Laboratory, Stanford University, from 2012 to 2014, and with the University of Malaga, from 2014 to 2015. He was a Visiting Researcher with the University College London, in 2010, and Queen's University Belfast, in 2018. Since 2015, he has been a Faculty Member with the Communication Engineering Department, University of Malaga, where he is currently an Associate Professor. His research interests include a diverse set of topics in the wide areas of communication theory and wireless communications, including stochastic processes, wireless channel modeling, physical layer security, and wireless powered communications. He has received several research awards, including the Best Paper Award from the Communication Theory Symposium at the IEEE GLOBECOM 2013, the IEEE Communications Letters Exemplary Reviewer Certificate, in 2014 and 2019, and the IEEE Transactions on Communications Exemplary Reviewer Certificate, in 2014, 2016, and 2019, respectively. He is an Editor of the IEEE Transactions on Communications, in the area of wireless communications.